THE JOURNAL OF BIOLOGICAL CHEMISTRY
Vol. 271, No. 24, Issue of June 14, pp. 14134–14142, 1996
Printed in U.S.A.

Specific Interaction of Glyceraldehyde 3-Phosphate Dehydrogenase with the 5′-Nontranslated RNA of Hepatitis A Virus*

(Received for publication, January 18, 1996, and in revised form, March 27, 1996)

Derk E. Schultz‡, Charles C. Hardin§, and Stanley M. Lemon‡¶

From the ‡Departments of Medicine and Microbiology and Immunology, The University of North Carolina at Chapel Hill, Chapel Hill, North Carolina 27599-7030 and the §Department of Biochemistry, North Carolina State University, Raleigh, North Carolina 27695-7622

Initiation of translation of hepatitis A virus (HAV) RNA occurs by internal entry and is likely to involve the interaction of trans-acting cellular protein factors with cis-acting structural elements of an internal ribosomal entry segment (IRES) within the 5′-nontranslated RNA. To characterize interactions between African green monkey kidney (BS-C-1) cell proteins and the predicted stem-loop IIIa (nucleotides 155–235) located at the 5′ border of the HAV IRES, we utilized an electrophoresis mobility shift assay (EMSA) to identify a 39-kDa RNA-binding protein (p39). Amino-terminal amino acid sequencing of highly purified p39 revealed absolute identity with human glyceraldehyde 3-phosphate dehydrogenase (GAPDH). The identity of p39 as simian GAPDH was further confirmed by antigenic and biochemical similarities between p39 and human GAPDH. Analysis of the RNA binding properties of simian GAPDH revealed that this cellular protein interacts with two additional sites in the HAV 5′-nontranslated RNA, one located between nucleotides 1–148 and the other between nucleotides 597–746. Competitive EMSAs also demonstrated that GAPDH and human polypyrimidine tract-binding protein, a putative picornavirus translation initiation factor, compete with each other for binding to stem-loop IIIa, suggesting that the relative cytoplasmic abundance of GAPDH and polypyrimidine tract-binding protein in individual cell-types may be an important determinant of viral translation activity. Human GAPDH was found to destabilize the folded structure of the stem-loop IIIa RNA based upon observed decreases in the circular dichroism spectra of this RNA following binding of the protein. This RNA helix-destabilizing activity of GAPDH could directly influence IRES-dependent translation and/or replication of picornavirus RNA.

Human hepatitis A virus (HAV),[1] an hepatovirus of the Picornaviridae family, is a positive-strand RNA virus with a genome length of approximately 7,480 nucleotides (1–3). The RNA genome is organized as a relatively long 734-nt 5′-nontranslated region (5′NTR), a single large open reading frame encoding the viral polyprotein, and a short 3′-nontranslated region. Among HAV strains, the 5′NTR is the most conserved region within the genome and contains extensive secondary and tertiary RNA structure (4). The highly ordered 5′NTR contains an internal ribosomal entry segment (IRES), located between nt 152 and the first initiator AUG at nt 735 in the HM175 strain, which regulates initiation of translation of the viral polyprotein by a cap-independent mechanism (5, 6). Compared with other picornaviruses, HAV IRES-directed translation is extremely inefficient, a feature that may contribute to the generally slow and noncytolytic replication of the virus in cell culture (5–7). In addition to its role in translation, it is likely that the 5′NTR also contains regulatory elements for initiation of positive-strand RNA synthesis (8) and possibly encapsidation of genomic RNA.

The cap-independent initiation of translation is an important aspect of HAV replication, strongly influencing the growth of the virus in cell culture and probably contributing to its pathogenicity in primates. Attenuated, cell culture-adapted strains of HAV have mutations from the wild-type sequence throughout the RNA genome, but these are concentrated in the 5′NTR as well as the P2 and P3 regions of the viral RNA, which encode nonstructural proteins involved in RNA replication (1, 9). Compared with wild-type virus, these attenuated viruses demonstrate enhanced growth in cultured cells but reduced growth in primary chimpanzee hepatocytes.[2] Although mutations in the P2 region are particularly important for cell culture-adaptation, studies of chimeric viruses containing 5′NTR sequences from wild-type or cell culture-adapted HAVs indicate that several mutations in the 5′NTR (at nt 152 and/or 203–204 and at nt 687) enhance viral growth in African green monkey kidney (BS-C-1) cells but not fetal rhesus monkey kidney (FRhK-4) cells (10–12). Furthermore, recent studies have shown that two of these mutations, a UU deletion at nt 203–204 of stem-loop IIIa of the 5′NTR and a U-to-G substitution in stem-loop V, act to enhance IRES-directed translation with a cell-type specificity consistent with their effects on viral replication (7).

The cap-independent translation of the HAV polyprotein, as well as that of other picornaviruses, is likely to be dependent upon the interaction of trans-acting host cell proteins with the cis-acting IRES located within the 5′NTR. This hypothesis is supported by several observations in addition to the cell-type specific action of the HAV mutations described above. First, efficient poliovirus and rhinovirus translation in rabbit reticulocytes lysate is dependent upon supplementation of the rabbit reticulocytes lysate with ribosomal salt wash (RSW) fractions

* This work was supported by Grants RO1-AI32599, T32-AI07151, and GM47431 from the United States Public Health Service. The costs of publication of this article were defrayed in part by the payment of page charges. This article must therefore be hereby marked "*advertisement*" in accordance with 18 U.S.C. Section 1734 solely to indicate this fact.

This paper is dedicated to the memory of Ki Ha Chang, Ph.D., who first recognized the viral RNA binding activities of the p39 protein.

¶ To whom correspondence should be addressed: Tel.: 919-966-2536; Fax: 919-966-6714.

[1] The abbreviations used are: HAV, hepatitis A virus; nt, nucleotide(s); IRES, internal ribosomal entry segment; RSW, ribosomal salt wash; GAPDH, glyceraldehyde 3-phosphate dehydrogenase; mAb, monoclonal antibody; EMSA, electrophoresis mobility shift assay; PAGE, polyacrylamide gel electrophoresis; PTB, polypyrimidine tract-binding protein; NTR, nontranslated region.

[2] S. F. Chao, R. E. Lanford, and S. M. Lemon, unpublished results.

from HeLa cells (13). Similarly, it has been suggested that HAV IRES-directed translation in rabbit reticulocytes lysate is enhanced following supplementation with cytoplasmic extracts from mouse liver (14). Finally, no picornavirus IRES has been reported to function in a wheat germ translation system, suggesting the absence of necessary trans-acting factors. Multiple cellular proteins, mostly derived from HeLa cells, have been shown to interact with picornavirus 5′NTRs. A 52-kDa nuclear autoantigen, La, binds with specificity to the poliovirus 5′NTR and appears to be the HeLa cell factor responsible for correcting aberrant translation of poliovirus RNA in rabbit reticulocyte lysates (15, 16). The 57-kDa polypyrimidine tract-binding protein (PTB), which may have a role in nuclear pre-mRNA splicing, also binds to several picornavirus 5′NTRs, including that of HAV (17–22). Recent studies, in which PTB was depleted from translationally active HeLa and Krebs-2 cell extracts, suggest that PTB may also have a role in picornavirus translation in these cell types (18, 23). Other identified cellular proteins that bind to the 5′NTRs of picornaviruses include the eucaryotic translation initiation factor, eIF-2A, and the elongation factor EF-1a (24, 25). Indeed, it is likely that all of the canonical translation initiation factors, with the possible exception of eIF-4f, are required for IRES-directed initiation of picornavirus translation, in addition to the novel putative translation factors mentioned above.

In previous studies, we utilized a UV cross-linking/label transfer assay to identify proteins of 30, 39, and 110 kDa (p30, p39, and p110), which are present in RSW prepared from HAV-permissive monkey kidney cells (BS-C-1 and FRhK-4) and which interact specifically with various RNA structural elements of the HAV and EMCV IRES elements (19). Here, we describe the purification of the BS-C-1 cell p39 protein and its identification as simian glyceraldehyde 3-phosphate dehydrogenase (GAPDH) based on amino-terminal microsequencing and antigenic relatedness to human GAPDH. As a tetramer of identical 37-kDa subunits, GAPDH is an important glycolytic enzyme that utilizes NAD^+ for the oxidative phosphorylation of glyceraldehyde 3-phosphate to 1,3-diphosphoglycerate (26, 27). Although previous studies also have shown GAPDH to be a nucleic acid-binding protein and to possess specific DNA repair activity, there are no previous reports of its interaction with viral RNAs. In this study, we characterize the interaction of GAPDH with stem-loop IIIa and other structural elements of the HAV 5′NTR.

MATERIALS AND METHODS

Reagents—Monoclonal antibody (mAb) 40.10.09 to human uracil-DNA glycosylase/GAPDH was kindly provided by Michael Sirover (Temple University School of Medicine, Philadelphia, PA). Goat anti-mouse IgG+IgA+IgM and alkaline phosphatase-conjugated anti-mouse IgG+IgA+IgM were purchased from BRL. Anti-HAV mAb 1.193 has been described previously (28). Human erythrocyte GAPDH, ribohomopolymers, and NAD^+ were purchased from Sigma. Recombinant human PTB was a gift from Mariano Garcia-Blanco (Duke University, Durham, NC). Sephacryl S-300 HR, DEAE Sephacel, and heparin-Sepharose were purchased from Pharmacia Biotech Inc., and [α-^{32}P]CTP (800 Ci/mmol) was obtained from Dupont NEN.

Plasmids—All HAV plasmid constructs contained sequences of the HM175/P16 strain of HAV (9) placed downstream of the promoter for bacteriophage T7 RNA polymerase. The numbering of HAV nucleotides in these constructs is based on the genome of the related wild-type virus (29). pHAV-s3a was constructed by polymerase chain reaction amplification of a 96-base pair fragment (HAV nt 155–235) flanked by 5′- and 3′-terminal *Eco*RI and *Xba*I sites from pLUC-P16-CAT (7) using the sense primer 5′-AATATGAATTCCTGCAGGTTCAGG-3′ and the antisense primer 5′-GCAATCTAGACCCTGGAAGAAAGAAGAC-3′. The resulting polymerase chain reaction fragment was digested with *Eco*RI and *Xba*I and subcloned into pGEM3Zf(−). pHAV-s5 was similarly constructed by polymerase chain reaction amplification of a 179-base pair fragment (HAV nt 596–746) using the sense primer 5′-GTGCTGAATTCAAACATCATTTGGCCTT-3′ and the antisense primer 5′-GCAATCTAGACCCTGGAAGAAAGAAGAC-3′. pHAV-Δ248, which contains nt 249–746 of the HAV genome, was constructed by digesting pHAV-CAT1 (6) with *Hin*dIII and *Avr*II. The resulting DNA was made blunt ended with Klenow fragment of *E. coli* DNA polymerase I, and the large fragment was isolated and religated. To confirm the sequences of the manipulated regions within the plasmids described above, DNAs were sequenced on a Model 373A DNA Sequencer (Applied Biosystems) using the *Taq* DyeDeoxy™ Terminator Cycle Sequencing Kit (Applied Biosystems).

RNA Transcription—For synthesis of RNA probes by run-off transcription, purified plasmid DNA was digested with restriction enzymes as follows: pHAV-CAT1, *Ssp*I (HAV nt 1–148); pHAV-s3a, *Xba*I (HAV nt 155–235); pHAV-Δ248, *Bam*HI (HAV nt 249–532); pHAV-s5, *Xba*I (HAV nt 596–746); and pGEM-3Zf(−), *Pvu*II (269 nt of a control transcript representing vector sequence). Transcription reactions were performed with T7 RNA polymerase (Promega) and [α-^{32}P]CTP (800 Ci/mmol) using Riboprobe System II reagents (Promega). Following transcription, reaction mixtures were digested with RQ1 RNase-free DNase (Promega) at 37 °C for 15 min. Transcripts were then phenol/chloroform extracted and ethanol precipitated and resuspended in buffer A (20 mM HEPES, pH 7.9, 1.5 mM $MgCl_2$, 10% glycerol (v/v), 0.5 mM dithiothreitol) with 25 mM KCl for binding assays. For analysis by circular dichroism (CD) spectropolarimetry, resuspended RNA representing HAV nt 155–235 was dialyzed extensively against 10 mM sodium phosphate, 10 mM KCl, 10% glycerol (v/v), 0.1 mM EDTA, 0.5 mM dithiothreitol.

Electrophoresis Mobility Shift Assay—EMSA conditions were adapted from Luo and Shuman (30) and Houser-Scott *et al.* (31). Binding reaction mixtures (10 μl) containing 0.2–1 pmol radiolabeled probe, 2 μg of yeast tRNA, and 0.5 unit of RNasin in buffer A with 25 mM KCl were incubated with protein for 10 min at room temperature. In experiments with purified p39 or human GAPDH (Sigma), the amount of protein added to the binding reaction was 0.1–0.5 pmol. When unlabeled competitor RNA or monoclonal antibody (25 ng) were included, they were added to the reaction mixture prior to the addition of p39 or human GAPDH. Following a 10-min incubation at room temperature, samples were electrophoresed through a native 4% polyacrylamide gel containing 0.25 × TBE (22.5 mM Tris borate, 0.5 mM EDTA). Electrophoresis was performed at room temperature at 125 V until the bromphenol blue marker had migrated approximately 7.5 cm into the gel. Labeled RNA was detected by autoradiography of the dried gel.

Preparation of BS-C-1 Cytoplasmic Extract—S100 extract was prepared from BS-C-1 cells as described by Chang *et al.* (19). Briefly, BS-C-1 cells (10 × 900 cm^2 roller bottles) were grown to 85% confluency and harvested mechanically. Cells were washed five times with ice-cold phosphate-buffered saline and collected by centrifugation at 150 × *g* for 10 min. The cell pellet was resuspended in 10.5 ml of hypotonic lysis buffer (10 mM HEPES, pH 7.9, 10 mM KCl, 1.5 mM $MgCl_2$, 0.5 mM dithiothreitol, and 0.1 mM phenylmethylsulfonyl fluoride) and homogenized by 50 strokes in a Dounce homogenizer. The suspension was centrifuged at 4,300 × *g* for 10 min to remove nuclei, and the resulting supernatant was centrifuged at 100,000 × *g* for 1 h. The buffer composition of the final supernatant (S100) was then adjusted to buffer A with 10 mM KCl.

Size Exclusion Chromatography of the BS-C-1 S100 Extract—BS-C-1 S-100 fraction (0.2 ml) was applied to a Sephacryl S-300 HR column (9 × 1.5 cm^2) equilibrated in buffer A with 25 mM KCl. Fractions (0.4 ml) were collected at a flow rate of 5 ml/h, and 5-μl aliquots of fractions were analyzed by EMSA as described above.

Purification of BS-C-1 p39—BS-C-1 S100 extract (9.5 ml) was applied to a DEAE-Sephacel column (5 × 1.5 cm^2) that had been equilibrated in buffer A with 10 mM KCl. The flow-through fraction was collected at a flow rate of 20 ml/h, and the column was eluted with 30 ml of buffer A containing 0.5 M KCl. The flow-through fraction from the DEAE-Sephacel was applied to a heparin-Sepharose column (2.5 × 1 cm^2) that had been equilibrated in buffer A containing 10 mM KCl. The column was eluted with 35 ml of a linear gradient of KCl (10–400 mM) gradient in buffer A. Fractions (1.0 ml) were collected at a flow rate of 10 ml/h. Fractions 12–15, which contained the majority of the HAV stem-loop IIIa binding activity (see "Results") were pooled and dialyzed against buffer A containing 25 mM KCl.

Amino Acid Sequencing—Protein from the pooled heparin-Sepharose chromatography fractions was acetone precipitated, electrophoresed on a 12% SDS-polyacrylamide gel, and electrotransferred to a polyvinylidene difluoride membrane in 25 mM Tris, pH 8.3, 192 mM glycine, 10% methanol. Protein bands were visualized by Coomassie Brilliant Blue staining, and the primary band corresponding to p39 was excised. For

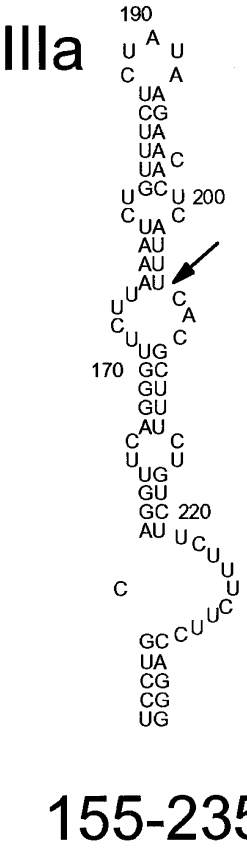

FIG. 1. **Proposed secondary structure of stem-loop IIIa within the 5′NTR of HM175/P16 virus is supported by analysis of covariant substitutions in different HAV strains and by probing the structure with single and double-strand-specific nucleases (4, 37).** Nucleotide positions are based upon the wild-type virus numbering (28). The *arrow* denotes the position of two U residues (nominally, nt 203–204) that are deleted from the wild-type sequence and that reduce the size of a bulge loop. The bases shown represent the HAV sequence present in the stem-loop IIIa RNA probe (nt 155–235).

amino-terminal sequencing, p39 (56 pmol) was analyzed on a gas-phase protein sequencer (Applied Biosystems 475A). Identification of proteins with regions homologous to the amino-terminal peptide of p39 was performed using the BLAST program (32).

Immunoblot Analysis—BS-C-1 p39 and human erythrocyte GAPDH (Sigma) were electrophoresed on a 12% SDS-polyacrylamide gel and subsequently transferred electrophoretically to a polyvinylidene difluoride membrane in 25 mM Tris, pH 8.3, 192 mM glycine, 10% methanol. Immunoreactive bands were identified following successive incubations with anti-uracil DNA glycosylase/GAPDH mAb 40.10.09 and alkaline phosphatase-conjugated goat anti-mouse IgG+IgA+IgM. Detection was performed with a BCIP/NBT color development system (Promega).

UV Cross-linking of RNA-Protein Complexes—The UV cross-linking reaction was performed essentially as described by Chang *et al.* (19) with some modifications. RNA binding mixtures contained ^{32}P-labeled RNA probe (HAV nt 155–235, 0.1 pmol/μl), 2 μg/μl yeast tRNA, and protein in buffer A with 25 mM KCl. Following a 10-min incubation at room temperature, samples were transferred to ice and irradiated for 20 min with a UV light source (254 nm 5.3 W: Phillips G10T5–1/2L lamp) at a distance of approximately 4 cm. After irradiation, RNA was digested with 1 μg/μl of RNase A and 0.1 unit/μl of RNase T1 for 20 min at 37 °C. The UV cross-linked products were separated on a 12% SDS-polyacrylamide gel and subsequently detected by autoradiography of the dried gel.

Immunoprecipitation of UV Cross-linked GAPDH—0.3 μg of p39 or human GAPDH were UV cross-linked with labeled HAV RNA as described above in a 50-μl volume. The reaction mixtures were diluted to 325 μl in NTE-40 buffer (50 mM Tris-HCl, pH 7.5, 150 mM NaCl, 1 mM EDTA, 0.1% Nonidet-40) and divided into three 100-μl aliquots. 250 ng of mAb to human GAPDH (40.10.09) or control mAb to HAV (1.193) was incubated with aliquots from both the p39 and human GAPDH UV cross-linking reactions. After a 1-h incubation at 4 °C, goat anti-mouse IgG+IgA+IgM, and protein G-Sepharose beads (Calbiochem) were added to reaction mixtures with occasional mixing for 1 h at 4 °C. Beads were pelleted by centrifugation, and supernatants were collected. Beads were washed three times with 1 ml of NTE-40 buffer, whereas supernatants were acetone precipitated. Samples were heated to 90 °C in Laemmli SDS sample buffer and analyzed by 12% SDS-PAGE.

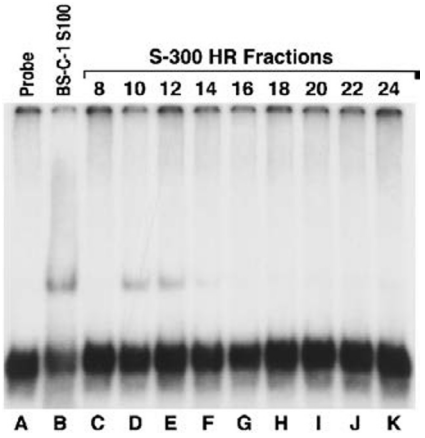

FIG. 2. **EMSA of BS-C-1 S100 preparation following fractionation by Sephacryl S-300HR chromatography.** Protein fractions were incubated with the uniformly labeled HAV stem-loop IIIa probe (Fig. 1) and electrophoresed on a 4% nondenaturing gel as described under "Materials and Methods." Molecular standards peaked at the following fractions: blue dextran, 8; aldolase (158 kDa), 11; bovine serum albumin (66.2 kDa), 15; and ovalbumin (42.7 kDa), 17. *Lane A*, stem-loop IIIa probe; *lane B*, probe plus S100 fraction; *lanes C–K*, probe plus S-300 HR column fractions.

Circular Dichroism—Measurements of CD spectra were performed with a Jasco J-600 spectropolarimeter interfaced to an IBM PC microcomputer as described previously (33). Temperature was maintained by placing the sample (800 μl) in a 1-cm path length cylindrical cell surrounded by an external jacket that was connected to a NesLab recirculating water bath. To correct for baseline signals due to the cell and buffer, CD spectra were normalized to 0 at a wavelength of 340 nm.

RESULTS

Identification of a BS-C-1 Cytoplasmic Factor That Interacts with Stem-loop IIIa of the HAV 5′NTR—Potential interactions between proteins present in RSW or cytoplasmic extract prepared from HAV-permissive BS-C-1 cells and an RNA probe representing stem-loop IIIa of the 5′NTR of HM175/P16 virus (Fig. 1) were examined in an EMSA. This RNA segment represents the most 5′ stem-loop within the IRES of HAV, as indicated by the fact that deletion of this stem-loop but not upstream RNA sequence significantly reduces the efficiency of internal initiation from bicistronic RNA transcripts (5, 8). Furthermore, deletion of a UU dinucleotide at nt 206–207, located within a bulge loop of this RNA (Fig. 1), has recently been shown to enhance translation of the viral RNA in BS-C-1 cells (7). For these experiments, synthetic stem-loop IIIa RNA was uniformly labeled with [^{32}P]CTP and incubated with either the RSW fraction or the cytoplasmic extract in the presence of yeast tRNA (200 μg/ml) as a nonspecific competitor. Electrophoresis of the reaction mixtures on a 4% nondenaturing polyacrylamide gel revealed retarded RNA-protein complexes with similar mass, suggesting that the RNA binding factor(s) present in these two cell fractions may be identical (Fig. 2, *lane B*, and data not shown). Binding of this factor(s) was inhibited in the presence of 0.1% SDS, suggesting that the factor is a protein and not nucleic acid (data not shown).

To determine the approximate molecular mass(es) of the protein(s) that binds to the stem-loop IIIa RNA, the BS-C-1 cytoplasmic extract was fractionated on a Sephacryl S-300 HR gel filtration column and fractions were assayed by EMSA. Under these conditions, the binding factor producing the re-

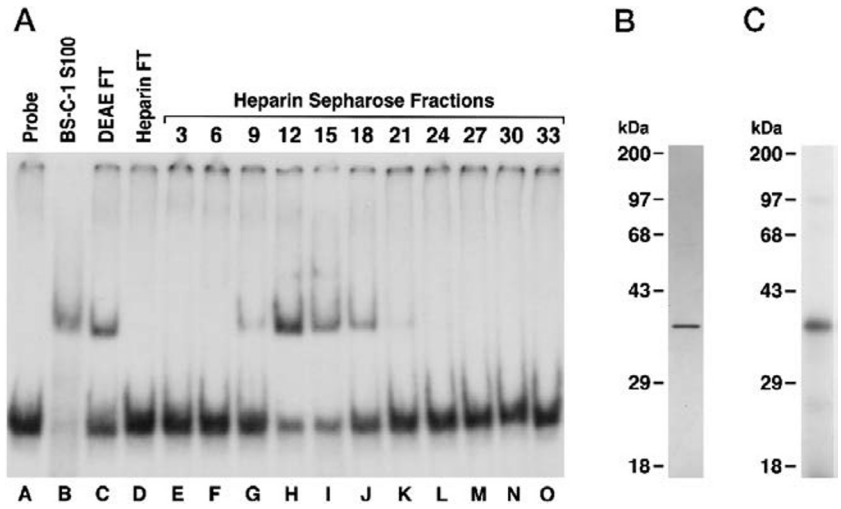

FIG. 3. **Isolation of a 39-kDa protein that binds to HAV stem-loop IIIa RNA.** *A*, BS-C-1 S100 fraction was applied to a DEAE-cellulose anion exchange column and the flow-through fraction was further fractionated by heparin-Sepharose chromatography as described under "Materials and Methods." Fractions were assayed by EMSA for their stem-loop IIIa binding activity. *Lane A*, labeled stem-loop IIIa RNA probe. *Lanes B-O* contain RNA incubated with BS-C-1 S100 fraction (*lane B*), DEAE flow-through (*FT*) fraction (*lane C*); heparin-Sepharose flow-through fraction (*lane D*); and heparin-Sepharose elution fractions 3–33 (*lanes E–O*). *B*, heparin-Sepharose fractions 12–15 were pooled and further analyzed by 12% SDS-PAGE followed by silver staining. *C*, transfer of label from stem-loop IIIa RNA to a 39-kDa protein in the pooled heparin-Sepharose fractions following UV cross-linking and extensive RNase digestion.

tarded RNA-protein complex in the EMSA eluted as a high molecular weight species with an approximate mass of 150 kDa (Fig. 2, *lanes D* and *E*). Similar results were found upon fractionation of the RSW fraction on the Sephacryl S-300 HR column (data not shown). Previous results indicate that BS-C-1 proteins of 30 and 39 kDa are the major proteins present in S100 or RSW fractions that UV cross-link to a similar HAV 5′NTR probe (19). These data thus suggested that either one or the other of these proteins exists as a high molecular weight complex in BS-C-1 cells. Alternatively, these data could be interpreted as showing a unique HAV RNA-binding protein that was not identified by the earlier UV cross-linking/label transfer assay employed by Chang *et al.* (19).

Purification and Amino-terminal Sequencing of the Cytoplasmic Factor That Binds to Stem-loop IIIa RNA—The ability to detect stem-loop IIIa RNA binding activity by EMSA following gel filtration chromatography suggested that EMSA could be utilized to monitor RNA binding activity following other chromatographic separation techniques. Thus, in an effort to purify the relevant RNA-binding factor, BS-C-1 cell cytoplasmic extract was applied to a DEAE-Sephacel column, and RNA binding activity was recovered in the flow-through fraction (Fig. 3*A*, *lane C*). This was followed by heparin-Sepharose chromatography, which resulted in a peak of RNA binding activity eluting at approximately 150 mM KCl (Fig. 3*A*, *lanes H* and *I*). Analysis of the pooled fractions (12–15) containing this peak binding activity by 12% SDS-PAGE followed by silver staining revealed a major protein band of 39 kDa that was approximately 85% pure (Fig. 3*B*). The UV cross-linking/label transfer assay using the pooled fractions also revealed a 39-kDa protein as the primary species to which ^{32}P label was transferred from the stem-loop IIIa RNA (Fig. 3*C*). Together, these data provided strong evidence that the 39-kDa protein was responsible for producing the RNA-protein complex in the fractions analyzed by EMSA. These data also suggest that p39 exists as part of a high molecular weight complex. It is likely that this 39-kDa protein is identical to p39, which we have previously shown to bind specifically to multiple sites within the HAV 5′NTR using the UV cross-linking/label transfer assay (19).

Following SDS-PAGE, the purified p39 protein was electroblotted onto a polyvinylidene membrane and subjected to amino-terminal amino acid sequencing with 27 rounds of Edman degradation. 25 of the first 27 amino acids of the 39-kDa protein were identical to the analogous residues of human GAPDH and a minor human uracil DNA glycosylase species, which recently has been shown to be the monomer subunit of GAPDH (34) (Table I). The nature of the remaining two residues of p39 (both Arg in GAPDH) could not be determined following Edman degradation. Human GAPDH is a tetrameric protein comprised of four 37-kDa monomers that plays an important role in glycolysis but that is multifunctional and interacts specifically with both tRNA and AU-rich eucaryotic mRNAs (35, 36).

TABLE I
Amino-terminal amino acid sequence of BS-C-1 p39 determined by amino-terminal sequencing and alignment with the sequence of an homologous peptide from human GAPDH

Protein	Amino acid sequence[a]	Position
BS-C-1 p39	GVKVGVNGFGXIGGXLVTRAAFNSG	
	|||||||||| ||| |||||||||	
Human GAPDH	GVKVGVNGFGRIGGRLVTRAAFNSG	2–28

[a] *X* denotes amino acid residues that could not be clearly identified in the Edman degradation.

Confirmation That the 39-kDa BS-C-1 RNA Binding Factor Is Simian GAPDH—To confirm that the RNA binding factor p39 is in fact GAPDH, a series of experiments were carried out comparing p39 and human erythrocyte GAPDH (Sigma). First, purified p39 and human GAPDH were probed in immunoblots with the anti-human uracil DNA glycosylase/GAPDH mAb 40.10.09 (Fig. 4*A*). As expected, the 40.10.09 mAb detected a single band of 37 kDa representing human GAPDH (Fig. 4*A*, *lane B*). In addition, the 40.10.09 mAb also recognized the BS-C-1 p39 protein, which migrated with a slightly higher apparent molecular mass than human GAPDH (Fig. 4*A*, *lane B*). Comparison of these two proteins by SDS-PAGE and silver staining also revealed this slight difference in apparent molecular mass (data not shown).

As with BS-C-1 p39, human GAPDH was found to be labeled after UV cross-linking with ^{32}P-labeled stem-loop IIIa RNA followed by extensive RNase digestion (Fig. 4*B*, *lanes A* and *F*). As additional evidence that p39 was in fact GAPDH, the resulting radiolabeled RNA-protein complexes could be immunoprecipitated with the anti-GAPDH 40.10.09 mAb but not with a control mAb directed against HAV capsid, 1.191 (Fig. 4*B*). Finally, purified GAPDH formed a primary complex with stem-loop IIIa RNA in EMSA, with a shift in mobility similar to the p39-RNA complex (Fig. 4*C*, *lanes B* and *E*). When the ratio of protein to stem-loop IIIa RNA was increased, a second minor RNA-protein complex with more retarded mobility formed with both p39 and GAPDH (data not shown). A very small amount of this secondary complex is apparent in Fig. 4*C* (*lanes B* and *G*). The addition of the 40.10.09 anti-GAPDH mAb further re-

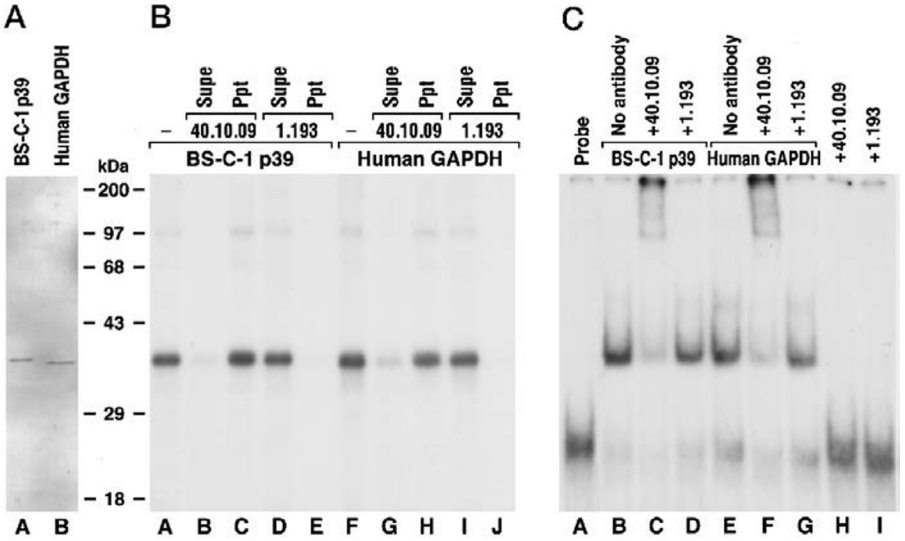

FIG. 4. **Antigenic relatedness of BS-C-1 p39 and human GAPDH.** *A*, immunoblot of purified BS-C-1 p39 (*lane A*) and human GAPDH (*lane B*) probed with mouse monoclonal anti-human GAPDH antibody 40.10.09. *B*, immunoprecipitation of UV cross-linked BS-C-1 p39 and human GAPDH. Purified p39 (*lanes A–E*) or human GAPDH (*lanes F–J*) were UV cross-linked to ^{32}P-labeled stem-loop IIIa RNA and extensively digested with RNases prior to SDS-PAGE. Labeled proteins (*lanes A* and *F*) were tested for their ability to be immunoprecipitated with anti-GAPDH monoclonal 40.10.09 (supernatant, *lanes B* and *G*; pellet *lanes C* and *H*) or control mouse monoclonal antibody to HAV capsid 1.193 (supernatant, *lanes D* and *I*; pellet, *lanes E* and *J*). *C*, mobility supershift of BS-C-1 p39-RNA and human GAPDH-RNA complexes with anti-GAPDH antibody. *Lane A*, labeled HAV stem-loop IIIa RNA probe. EMSA reactions contained RNA incubated with BS-C-1 p39 (*lanes B–D*) or human GAPDH (*lanes E–G*) in the presence of no antibody (*lanes B* and *E*), anti-GAPDH monoclonal 40.10.09 (*lanes C* and *F*), or control antibody 1.193 (*lanes D* and *G*). *Lanes H* and *I* represent probe reacted with antibody 40.10.09 (*lane H*) or 1.193 (*lane I*) in the absence of p39 or GAPDH.

tarded (supershifted) the migration of the major RNA-protein complex in EMSA reactions containing radiolabeled stem-loop IIIa RNA complexed to either BS-C-1 p39 or human GAPDH (Fig. 4*C*, *lanes C* and *F*). No such supershift was apparent with the control 1.191 mAb (Fig. 4*C*, *lanes D* and *G*), whereas addition of the 40.10.09 mAb to the RNA probe in the absence of either p39 or GAPDH also resulted in no shift (Fig. 4*C*, *lane H*).

The RNA binding properties of BS-C-1 p39 and human GAPDH were compared with each other to further confirm the identity of p39 as simian GAPDH. Nagy and Rigby (36) previously demonstrated that GAPDH binds RNA in its NAD^+ coenzyme binding site (otherwise known as the "Rossmann fold"). In competitive binding experiments with p39 or human GAPDH, NAD^+ inhibited binding of both proteins to stem-loop IIIa RNA at nearly identical concentrations (Fig. 5). In addition, various unlabeled ribohomopolymers competed with ^{32}P-labeled stem-loop IIIa RNA for binding with p39 or human GAPDH with approximately equal efficiencies (Fig. 6). As demonstrated previously in competitive binding experiments with the 3′NTR of the interferon-γ 3′ mRNA (36), poly(U) was the strongest competitor of RNA binding to GAPDH as well as the BS-C-1 p39 protein (Fig. 6, *lanes D* and *K*). A lesser degree of binding competition was observed at the highest concentration of poly(A), whereas poly(C) had no apparent effect on stem-loop IIIa binding to GAPDH or p39.

Specificity of Simian GAPDH Binding to the HAV 5′NTR—To localize the binding sites of simian GAPDH (BS-C-1 p39) within the HAV 5′NTR and confirm previous observations of the specific binding of p39 to HAV RNA, we determined the ability of various unlabeled RNA probes representing different structural elements of the HAV 5′NTR to compete for binding to purified p39 in the UV cross-linking/label transfer assay. The unlabeled competitor probes are shown in Fig. 7*A* and included RNA transcripts corresponding to nt 1–148 (representing stem-loops I-IIb in addition to the most 5′ pyrimidine-rich tract, pY1), nt 155–235 (stem-loop IIIa), nt 249–632 (stem-loops IIIb-IV), and nt 596–744 (stem-loop V to the initiator AUG codon) (4, 37). In addition, a 269-nt transcript (GEM-t) derived from pGEM3Zf(−) was utilized as a

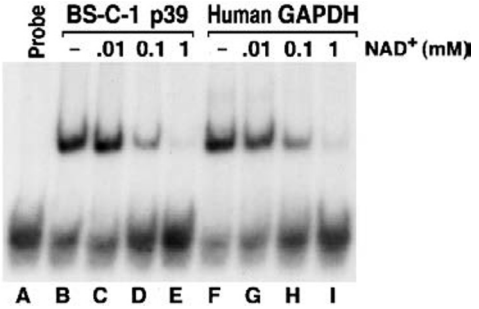

FIG. 5. **EMSA demonstrating competition between the coenzyme NAD^+ and stem-loop IIIa RNA for binding to purified BS-C-1 p39 and human GAPDH.** *Lane A*, labeled stem-loop IIIa RNA probe. EMSA reactions contained probe incubated with BS-C-1 p39 (*lanes B–E*) or human GAPDH (*lanes F–I*) in the absence of added NAD^+ (*lanes B* and *F*) or in the presence of 0.01 (*lanes C* and *G*), 0.1 (*lanes D* and *H*), or 1 mM NAD^+ (*lanes E* and *I*).

nonspecific competitor RNA in these experiments. In the UV cross-linking/label transfer assay, the 1–148 and 155–235 nt probes were the strongest competitors, followed by the 596–744 nt probe (Fig. 7*B*). Both the 249–632 nt HAV probe and the control GEM-t were relatively weak competitors showing little if any effect at molar concentrations 200-fold in excess of the radiolabeled stem-loop IIIa RNA. These data thus support the specific nature of the interaction between GAPDH and stem-loop IIIa RNA but confirm earlier observations that p39 (GAPDH) binds to several sites within the 5′NTR (19). Importantly, the three sites that specifically bound purified simian GAPDH in the UV cross-linking/label transfer assay did not differ from those that were previously found to bind the 39-kDa protein identified in a crude BS-C-1 cell extract (19). This provides further evidence that these proteins are identical. Because the 249–632-nt and 596–744-nt HAV RNA probes overlap each other by 37 nt, the low affinity GAPDH binding activity of the latter probe is likely to be located between nt 633 and 744 or to be dependent upon the presence of an intact stem-loop Va (4).

GAPDH and PTB Compete for Binding to HAV Stem-loop

IIIa—Several lines of evidence suggest that GAPDH and PTB, a putative picornavirus translation initiation factor (18, 21), have similar RNA binding specificities. This includes the similar binding specificity of these proteins for ribohomopolymers (36, 38) and previous observations suggesting that BS-C-1 p39 and HeLa cell p57 (PTB) compete for similar binding sites on the HAV 5′NTR (19). To determine whether GAPDH and PTB compete for binding to a functionally significant region of the HAV 5′NTR, we carried out UV cross-linking/label transfer assays with uniformly labeled stem-loop IIIa RNA and reaction mixtures containing both human GAPDH and PTB in varied molar ratios (Fig. 8). As expected, in reactions with GAPDH or PTB alone, the label was transferred to proteins of 37 or 57 kDa, respectively, with label transfer to PTB being more efficient than to GAPDH (Fig. 8, *lanes A* and *I*). However, in reactions with equimolar quantities of the two RNA-binding proteins, label transfer to GAPDH was significantly reduced, whereas label transfer to PTB was not impaired (Fig. 8, *lane E*). When the molar concentration of PTB was 10-fold higher than GAPDH, label transfer to GAPDH was not detected, whereas a 10-fold molar excess of GAPDH resulted in only a modest reduction of label transfer to PTB. These results are consistent with competition between GAPDH and PTB for binding to similar or overlapping sites on the stem-loop IIIa RNA and indicate that the binding affinity of PTB is substantially higher than that of GAPDH.

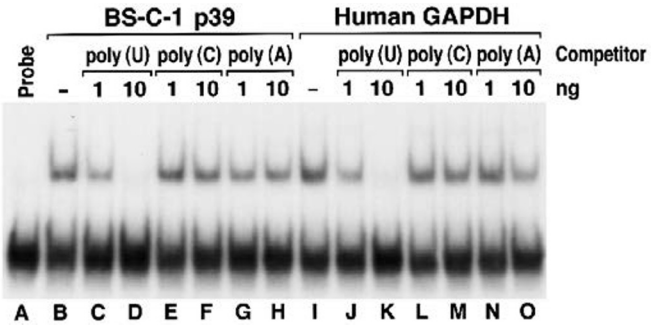

FIG. 6. **EMSA demonstrating competition between ribohomopolymers and stem-loop IIIa RNA for binding to BS-C-1 p39 and human GAPDH.** *Lane A*, stem-loop IIIa RNA probe. EMSA reactions contained probe incubated with BS-C-1 p39 (*lanes B–H*) or human GAPDH (*lanes I–O*) in the presence of no competitor (*lanes B* and *I*), 1 ng of poly(U) (*lanes C* and *J*), 10 ng of poly(U) (*lanes D* and *K*), 1 ng of poly(C) (*lanes E* and *L*), 10 ng of poly(C) (*lanes F* and *M*), 1 ng of poly(A) (*lanes G* and *N*), or 10 ng of poly(A) (*lanes H* and *O*).

Circular Dichroism Spectra of Stem-loop IIIa RNA Complexed with Human GAPDH—Previously, both yeast GAPDH and human GAPDH (P8 protein) were found to possess a helix destabilizing activity that could depress the melting temperature of poly(A-U) by as much as 28 and 24 °C, respectively (39). By definition, helix destabilizing proteins bind single-stranded polynucleotides with higher affinity than double-stranded helical polynucleotides, with the resulting equilibrium favoring the single-stranded conformation (40). A common experimental property of several helix destabilizing proteins, including yeast GAPDH and the prototype T4 bacteriophage gene 32 protein (39, 40), is that they affect a substantial decrease in the CD spectra of helical nucleic acids. This phenomenon has been interpreted as evidence for protein-induced melting of the polynucleotide helix accompanied by unstacking of nucleic acid bases.

To determine whether the reported helix-destabilizing activity of GAPDH extended to its interaction with stem-loop IIIa RNA, we examined the effect of GAPDH binding on the CD spectra of this RNA. Fig. 9*A* depicts the CD spectra of isolated stem-loop IIIa RNA in the absence of protein at temperatures

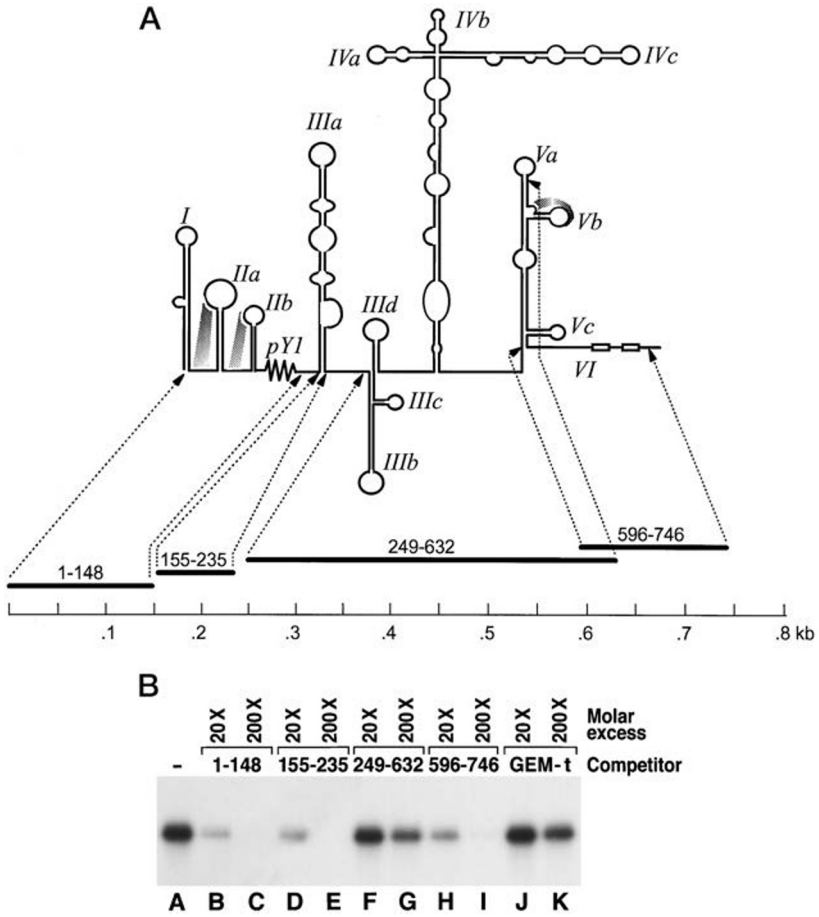

FIG. 7. **Competition between several unlabeled RNAs representing segments of the HAV 5′NTR and labeled stem-loop IIIa RNA for binding to BS-C-1 p39 (simian GAPDH).** *A*, predicted secondary and tertiary structure (4, 37) of the 5′NTR of HM175/P16 virus in the regions represented by unlabeled RNA probes 1–148, 249–632, and 596–746 used in competition experiments. Individual stem-loops are labeled I, IIa, etc., whereas pY1 denotes the 5′ pyrimidine-rich tract. Base pair interactions in putative pseudoknots are indicated by *shaded areas*. The two *boxes* indicate the initiator codons (1 and 3) at the 5′ end of the long ORF. Nucleotide numbering is that of the related wild-type virus (28). *B*, competitive UV cross-linking/label transfer reactions containing ^{32}P-labeled stem-loop IIIa RNA (Fig. 1) incubated with purified BS-C-1 p39 in the presence of a 20- or 200-fold molar excess of unlabeled synthetic RNAs representing various segments of the HAV 5′NTR (*lanes B–I*) or an unrelated 269-nt control RNA transcribed from pGEM3Zf(−) DNA linearized by digestion with *Pvu*II (*lanes J* and *K*). No RNA competitor was present in *lane A*.

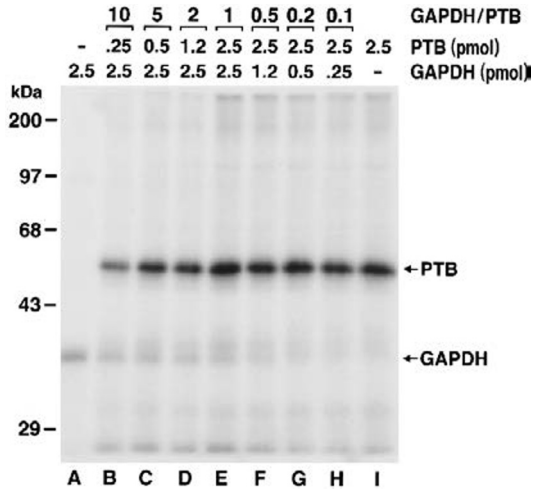

FIG. 8. **Competition between GAPDH and PTB for binding to labeled stem-loop IIIa RNA in a UV cross-linking/label transfer assay.** *Lane A* contains products of a UV cross-linking reaction with isolated GAPDH, whereas *lane I* contains products of UV cross-linking to PTB. *Lanes B–H* contain varying molar ratios of monomer GAPDH and PTB as indicated at the *top*. The molar quantities of human GAPDH (monomer) or human PTB in a 15-μl binding reaction are also indicated.

ranging from 10 to 80 °C. Inspection of these spectra reveals a positive band centered at approximately 268 nm, with a progressive reduction in the molar ellipticity between 250 and 290 nm with increasing temperatures. Because the structure of stem-loop IIIa RNA has previously been shown to have significant double-stranded character (4, 37), the reduction in intensity of the stem-loop IIIa RNA spectra with increasing temperature is likely to reflect disruption of base pair interactions that are present in the folded conformation of this RNA. Fig. 9*B* shows the CD spectra of stem-loop IIIa RNA (250 nM) at 15 °C in the presence of three different concentrations of human GAPDH (1, 2, and 4 μM), as well as the CD spectra of isolated human GAPDH at concentrations of 2 and 4 μM. The minimal ellipticity of isolated GAPDH at wavelengths greater than 250 nm (Fig. 9*B*) allowed a straightforward assessment of the effect of this protein on the CD spectra of the RNA between 250 and 290 nm. The addition of even low concentrations of GAPDH (1–2 μM) to stem-loop IIIa RNA resulted in a significant reduction in the intensity of the RNA spectra at wavelengths between 250 and 290 nm (Fig. 9*B*). This effect was dependent upon the concentration of GAPDH and resembled the reduction in ellipticity, which was observed upon thermal denaturation of the RNA (Fig. 9*A*). In contrast to GAPDH, the addition of a 10-fold molar excess of albumin to stem-loop IIIa RNA had no effect on the CD spectra of the RNA between 250 and 290 nm (data not shown). These data thus indicate that the binding of GAPDH to stem-loop IIIa RNA significantly destabilizes the secondary structure of this RNA, suggesting that GAPDH binds the single-stranded RNA with greater affinity than helical segments of this stem-loop or that it converts helical segments to unpaired strands.

Fig. 9*C* shows the molar ellipticity of RNA-GAPDH mixtures at the peak wavelength (268 nm) as a function of the molar ratio of monomeric GAPDH to stem-loop IIIa RNA (held constant at 250 nM) (molar ellipticity normalized for the spectral contribution of GAPDH). These results show that a molar ratio of monomeric GAPDH to RNA of approximately 4:1 is required for a half-maximal change in the RNA structural perturbation. If GAPDH is predominantly tetrameric under the conditions of this experiment, these results would suggest that a ratio of one GAPDH tetramer/RNA molecule is required for half-maximal

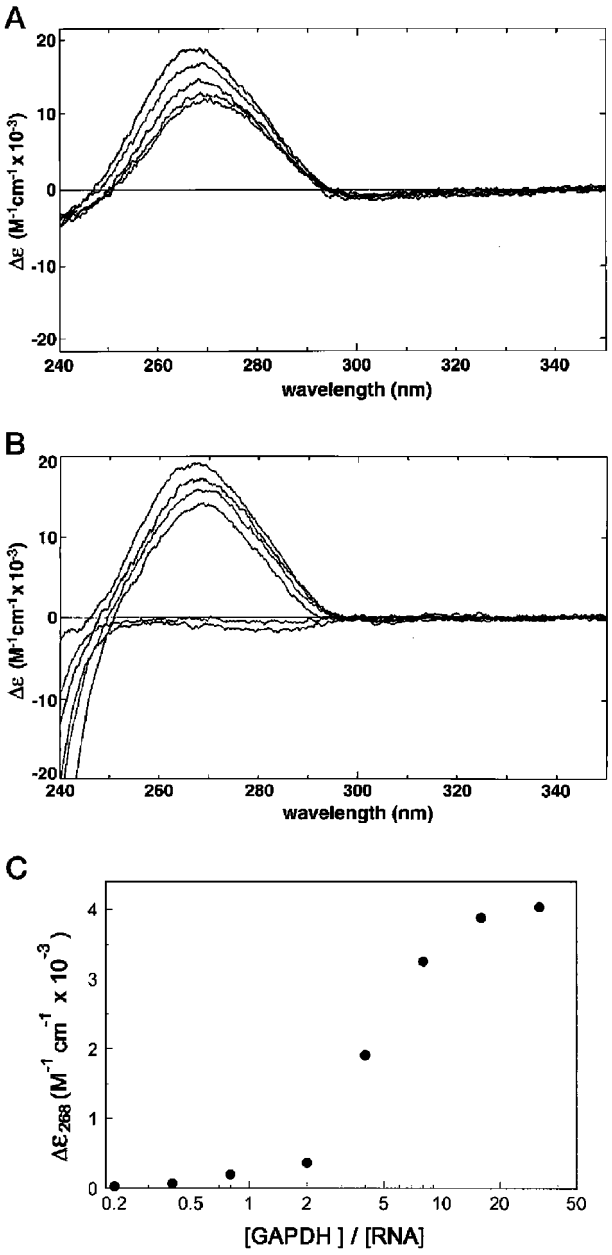

FIG. 9. **CD spectropolarimetry of stem-loop IIIa RNA in the presence and absence of GAPDH.** Spectra were obtained in 10 mM $NaPO_4$, pH 7.7, 10 mM KCl, 0.1 mM Na_2EDTA, 0.5 mM dithiothreitol, 10% glycerol. *A*, CD spectra obtained during progressive thermal denaturation of stem-loop IIIa RNA (concentration, 225 nM) at 10, 30, 40, 50, and 80 °C. The molar ellipticity values in the 250–280 nm range decreased as the temperature was increased. *B*, the effect of human GAPDH on the CD spectra of stem-loop IIIa RNA. Spectra shown were obtained at 15 °C with stem-loop IIIa RNA (concentration, 250 nM) and GAPDH (molar concentrations of the 37-kDa monomer equal to 0, 1, 2, and 4 μM). The molar ellipticity values in the 250–280 nm range decreased significantly as the concentration of GAPDH was increased. Spectra of GAPDH alone (2 and 4 μM concentrations) are also shown; molar ellipticity values in the 250–300 nM range with the protein alone are only slightly below the buffer baseline. Thus, the ellipticity observed in this range with the mixture of RNA and GAPDH is contributed almost exclusively from the RNA. *C*, the change in molar ellipticity of stem-loop IIIa RNA at 268 nm is plotted as a function of the molar ratio of monomeric GAPDH to RNA. Molar ellipticity values at GAPDH concentrations of 2, 4, and 8 μM were normalized for the molar ellipticity contribution of GAPDH at these concentrations.

destabilization of the RNA structure. However, although GAPDH is predominantly a tetrameric protein, further interpretation of these results is hindered by the fact that GAPDH

can exist as an equilibrium mixture of tetramers, monomers, and possibly dimers under conditions where the concentration of protein is relatively low, such as those described in Fig. 9*C* (41–43). Although the monomeric form of GAPDH has been reported to bind poly(dU) and to possess an associated uracil DNA glycosylase activity (34), it is still not clear which form(s) of GAPDH bind to RNA. Furthermore, it is also unknown whether GAPDH binding to RNA affects the relative abundance of tetramers, dimers, and monomers.

DISCUSSION

Although the precise mechanism by which picornavirus translation is initiated remains unknown, it is likely to depend upon the interaction of trans-acting cellular factors with cis-acting elements of the 5′NTR, which result in the binding of the 40 S ribosomal subunit at a position that is favorable for translation to be initiated at the proper AUG initiator codon. Studies that examined the translation of HAV RNA in rabbit reticulocyte lysates indicated that the HAV IRES is located between nt 151–735 of the 5′NTR (5). Interestingly, the 5′ border of the HAV IRES coincides with a stem-loop structure (domain IIIa), which suggests that base pairing in this region is important for IRES-directed translation (Figs. 1 and 7*A*) (4, 5, 37). Immediately 5′ of this stem-loop there is an extended single-stranded domain within which deletions do not significantly impair translation but do result in a temperature-sensitive replication phenotype due to a reduction in RNA synthesis (8, 37). Within stem-loop IIIa, a deletion of two U residues at nt 206–207, which normally contribute to a bulge-loop in this RNA, has been shown to enhance the growth of cell culture-adapted virus in continuously cultured African green monkey kidney (BS-C-1) cells due to a specific enhancement of IRES-dependent translation in these cells (7, 12). Thus, several independent lines of evidence indicate that stem-loop IIIa plays an important role in the initiation of HAV translation by internal entry.

Here, we show that a protein of approximately 39 kDa (p39), which is present in BS-C-1 cell cytoplasmic extracts and RSW fractions and which binds with relative specificity to stem-loop IIIa RNA, is simian GAPDH. The identification of this protein as GAPDH was based upon several comparisons of the purified p39 RNA-binding protein with human GAPDH, a tetrameric protein that is composed of four identical 37-kDa subunits (26, 27). First, amino-terminal amino acid sequencing of p39 revealed absolute identity between p39 and human GAPDH at the 25 amino acid residues that were identified in the first 27 cycles of Edman degradation (Table I). In addition, as with the BS-C-1 p39 protein, human GAPDH also was UV cross-linked in RNA binding reactions with radiolabeled stem-loop IIIa RNA and formed a complex with this RNA in EMSA that migrated in similar fashion to the p39-RNA complex in a nondenaturing acrylamide gel (Fig. 4). Furthermore, p39 and human GAPDH were found to be antigenically related based upon immunoblot analysis, immunoprecipitation of stem-loop IIIa RNA-protein complexes with anti-GAPDH monoclonal antibody, and a mobility supershift of this complex by anti-GAPDH antibody in EMSA (Fig. 4). Competition binding experiments with NAD^+ and the ribohomopolymers poly(U), poly(C), and poly(A) demonstrated strong similarities between p39 and human GAPDH (Figs. 5 and 6). Finally, because GAPDH exists primarily as a tetrameric protein (26, 27), the identification of p39 as simian GAPDH is also consistent with our finding that the RNA binding activity of p39 elutes from a size exclusion column with an apparent molecular mass of approximately 150 kDa (Fig. 2).

Previous studies have shown that GAPDH is an abundant, multifunctional enzyme that is primarily cytoplasmic but also present in the nucleus (35). In addition to its role in glycolysis, several unrelated activities have been attributed to GAPDH including DNA repair (34), protein phosphorylation (44), and interaction with RNA (35, 36), DNA (34, 45), microtubules (46), and red cell membranes (47). Similar to our finding that GAPDH binds to several regions within the HAV 5′NTR, GAPDH has been shown recently to bind to certain tRNAs and eucaryotic mRNAs (35, 36). It has been reported that GAPDH binds yeast $tRNA^{Ser}$ with an apparent dissociation constant (K_d) of approximately 1.8×10^{-8} M and other tRNAs with high affinity and has been suggested to participate in the export of tRNAs from the nucleus (35). Although we have not measured the K_d of GAPDH for different segments of the HAV 5′NTR in this study, it is not unreasonable to assume that it possesses an affinity for stem-loop IIIa RNA that is at least comparable with its affinity for yeast tRNAs, because these tRNAs were present at high concentration (200 μg/ml) as "nonspecific" competitors in our binding assays. Nagy and Rigby (36) have shown that GAPDH interacts specifically with AU-rich elements of mRNAs and have proposed that this interaction plays a role in regulating AU-rich elements-dependent mRNA translation. The AU-rich elements RNA binding region of GAPDH was localized to the NAD^+ binding domain or dinucleotide-binding (Rossmann) fold of the enzyme, consistent with our finding that binding of p39 or GAPDH to stem-loop IIIa RNA is inhibited by NAD^+ (Fig. 5).

Competitive binding experiments confirmed that GAPDH (p39) binds to multiple sites within the HAV 5′NTR. GAPDH was found to bind RNA probes representing nt 1–148, 155–235, and 596–746 but with greatest affinity to the nt 1–148 (which contains the pY1 pyrimidine-rich tract) and nt 155–235 (stem-loop IIIa) RNAs (Fig. 7). In previous UV cross-linking/label transfer studies, the 39-kDa protein present in BS-C-1 cell extracts was found to have similar binding specificities, which strongly suggests that our purified p39 is identical to this previously identified protein (19). GAPDH is thus similar to PTB in its interaction with the 5′NTR, because PTB also binds to multiple sites within the 5′NTRs of HAV and other picornaviruses (18–22). We previously found that p39 binds specifically to RNA probes representing the IRES of encephalomyocarditis virus, a picornavirus, as well as the 5′NTR of hepatitis C virus, a member of the Flaviviridae that also translates its polyprotein by an IRES-directed mechanism (19, 48, 49). In addition, in preliminary studies we have found that both simian GAPDH and human GAPDH interact with the poliovirus 5′ cloverleaf in a UV cross-linking/label transfer assay.[3] These data raise the possibility that GAPDH may be identical to a 36-kDa cellular protein of HeLa cells that has been implicated in promoting the binding of the poliovirus $3CD^{pro}$ protein to the 5′ end of the viral plus-strand RNA, in a step that is critically important for replication of the viral RNA (50). The affinity of GAPDH for the 5′NTRs of several different positive-strand RNA viruses suggests that it might contribute functionally to the replication of these viruses by one or more specific mechanisms.

Although we have not determined whether GAPDH plays a role in the replication of HAV, the ability of GAPDH to decrease the melting temperature of poly(A-U) (39) suggested that it might function to destabilize RNA structural elements that regulate translation initiation or RNA replication. In support of this hypothesis, we found that GAPDH specifically reduces the intensity of the circular dichroism spectra of stem-loop IIIa RNA (Fig. 9*B*), indicating that GAPDH binding favors the single-stranded form of this RNA over its predicted stem-loop conformation (Fig. 1). Because the functional activities of IRESs are strongly dependent upon their secondary RNA

[3] D. E. Schultz, and S. M. Lemon, unpublished results.

structure (51), it is tempting to speculate that the destabilization of stem-loop IIIa structure by GAPDH would adversely influence internal initiation of translation directed by the HAV IRES. However, different mechanisms can be envisioned whereby GAPDH could have a positive or negative impact on translation, depending upon whether the initial contact site of the 40 S ribosome subunit or translation initiation factors that might bind to the IRES in advance of the ribosome is a highly structured or single-stranded RNA conformation. Either way, it is important to note that the cytoplasmic abundance of GAPDH distinguishes it from the putative picornaviral translation initiation factors, La and PTB, which are predominantly nuclear proteins.

Although PTB has been suggested to function as a trans-acting factor in initiation of picornavirus translation (18, 23), it is interesting that BS-C-1 cells that are permissive for both HAV and poliovirus have extremely low levels of this protein compared with the levels found in HeLa cells (18, 19). Unlike PTB, GAPDH is expressed at relatively high levels in all living cells because of its important role in carbohydrate metabolism. We demonstrated that PTB and GAPDH compete with each other for binding to stem-loop IIIa of the HAV 5′NTR (Fig. 8). This suggests the interesting possibility that the functional role of PTB in IRES-directed translation may be to compete with and prevent the binding of GAPDH to the IRES with its attendant RNA helix destabilizing activity. Alternatively, binding of GAPDH to the 5′NTR could indirectly influence internal initiation of translation by limiting the interaction of the putative trans-acting factor PTB with structural elements of the IRES. In either case, the functional impact of interactions of GAPDH and PTB with picornavirus RNAs is likely to be dependent upon the relative abundance of these proteins within the cytoplasm of specific cell types. Thus, competition between PTB and GAPDH for identical or at least overlapping binding sites on viral RNA may contribute substantially to the cell type-specific differences in RNA-binding proteins that were identified previously in BS-C-1 and HeLa cell extracts (19).

It is interesting that the two mutations in the 5′NTR of the cell culture-adapted HM175/P16 virus that enhance IRES-directed translation in BS-C-1 cells (7), a UU deletion at position 203–204 and a U-to-G substitution at position 687, both remove uracil bases from potential GAPDH binding sites. Because GAPDH binding sequences are characteristically U-rich (Fig. 6) (36), such mutations would be predicted to reduce the affinity of the RNA for GAPDH. This line of reasoning is consistent with the hypothesis that binding of GAPDH to the HAV 5′NTR may be detrimental to IRES-directed translation and that these mutations might decrease this interaction in the low PTB environment of BS-C-1 cells and thereby enhance cap-independent viral translation. However, it should be noted that these mutations do not enhance viral translation in HAV-permissive FRhK-4 cells, which also have a very low abundance of PTB and have proteins of 30 and 39 kDa (GAPDH), which bind specifically to elements of the HAV IRES (7, 19).

Independent of translation, the interaction of GAPDH with the 5′ end of HAV RNA could also contribute to replication of the viral RNA. Although speculative, it is possible that the helix destabilizing activity of GAPDH could promote the dissociation of positive and negative strands of the replicative form RNA, thereby facilitating the separation of these strands, which is required for initiation of further rounds of positive-strand RNA synthesis (50). Alternatively, destabilization of secondary structure within the 5′NTR could facilitate the passage of the RNA replicase during synthesis of negative-strand RNA. Further experiments will be required to test these possibilities.

Acknowledgments—We thank Michael Sirover, Lee Gehrke, and Mariano Garcia-Blanco for helpful advice and for providing antibody against human uracil-DNA glycosylase/GAPDH (M. S.) and recombinant human PTB (M. G.-B.). We also thank Russell Henry and Matthew Corregan for their technical assistance.

REFERENCES

1. Cohen, J. I., Rosenblum, B., Ticehurst, J. R., Daemer, R. J., Feinstone, S. M., and Purcell, R. H. (1987) *Proc. Natl. Acad. Sci. U. S. A.* **84,** 2497–2501
2. Najarian, R., Caput, D., Gee, W., Potter, S. J., Renard, A., Merryweather, J., Van Nest, G., and Dina, D. (1985) *Proc. Natl. Acad. Sci. U. S. A.* **82,** 2627–2631
3. Lemon, S. M., and Robertson, B. H. (1993) *Semin. Virol.* **4,** 285–295
4. Brown, E. A., Day, S. P., Jansen, R. W., and Lemon, S. M. (1991) *J. Virol.* **65,** 5828–5838
5. Brown, E. A., Zajac, A. J., and Lemon, S. M. (1994) *J. Virol.* **68,** 1066–1074
6. Whetter, L. E., Day, S. P., Elroy-Stein, O., Brown, E. A., and Lemon, S. M. (1994) *J. Virol.* **68,** 5253–5263
7. Schultz, D. E., Honda, M., Whetter, L. E., McKnight, K. L., and Lemon, S. M. (1996) *J. Virol.* **70,** 1041–1049
8. Shaffer, D. R., and Lemon, S. M. (1995) *J. Virol.* **69,** 6498–6506
9. Jansen, R. W., Newbold, J. E., and Lemon, S. M. (1988) *Virology* **163,** 299–307
10. Emerson, S. U., Huang, Y. K., McRill, C., Lewis, M., and Purcell, R. H. (1992) *J. Virol.* **66,** 650–654
11. Emerson, S. U., Huang, Y. K., and Purcell, R. H. (1993) *Virology* **194,** 475–480
12. Day, S. P., Murphy, P., Brown, E. A., and Lemon, S. M. (1992) *J. Virol.* **66,** 6533–6540
13. Brown, B. A., and Ehrenfeld, E. (1979) *Virology* **97,** 396–405
14. Glass, M. J., and Summers, D. F. (1993) *Virology* **193,** 1047–1050
15. Meerovitch, K., Svitkin, Y. V., Lee, H. S., Lejbkowicz, F., Kenan, D. J., Chan, E. K. L., Agol, V. I., Keene, J. D., and Sonenberg, N. (1993) *J. Virol.* **67,** 3798–3807
16. Meerovitch, K., Pelletier, J., and Sonenberg, N. (1989) *Genes & Dev.* **3,** 1026–1034
17. Garcia-Blanco, M. A., Jamison, S. F., and Sharp, P. A. (1989) *Genes & Dev.* **3,** 1874–1886
18. Hellen, C. U. T., Witherell, G. W., Schmid, M., Shin, S. H., Pestova, T. V., Gil, A., and Wimmer, E. (1993) *Proc. Natl. Acad. Sci. U. S. A.* **90,** 7642–7646
19. Chang, K. H., Brown, E. A., and Lemon, S. M. (1993) *J. Virol.* **67,** 6716–6725
20. Luz, N., and Beck, E. (1991) *J. Virol.* **65,** 6486–6494
21. Hellen, C. U. T., Pestova, T. V., Litterst, M., and Wimmer, E. (1994) *J. Virol.* **68,** 941–950
22. Borman, A., Howell, J. G., Patton, J. G., and Jackson, R. J. (1993) *J. Gen. Virol.* **74,** 1775–1778
23. Borovjagin, A., Pestova, T., and Shatsky, I. (1994) *FEBS Lett.* **351,** 299–302
24. Del Angel, R. M., Papavassiliou, A. G., Fernandez-Thomas, C., Silverstein, S. J., and Racianello, V. R. (1989) *Proc. Natl. Acad. Sci. U. S. A.* **86,** 8299–8303
25. Harris, K. S., Xiang, W., Alexander, L., Lane, W. S., Paul, A. V., and Wimmer, E. (1994) *J. Biol. Chem.* **269,** 27004–27014
26. Harrington, W. F., and Karr, G. M. (1965) *J. Mol. Biol.* **13,** 885–893
27. Harris, J. I., and Perham, R. N. (1965) *J. Mol. Biol.* **13,** 876–884
28. Ping, L.-H., and Lemon, S. M. (1992) *J. Virol.* **66,** 2208–2216
29. Cohen, J. I., Ticehurst, J. R., Purcell, R. H., Buckler-White, A., and Baroudy, B. M. (1987) *J. Virol.* **61,** 50–59
30. Luo, Y., and Shuman, S. (1993) *J. Biol. Chem.* **268,** 21253–21262
31. Houser-Scott, F., Baer, M. L., Liem, K. F., Cai, J.-M., and Gehrke, L. (1994) *J. Virol.* **68,** 2194–2205
32. Altschul, S. F., Gish, W., Miller, W., Myers, E. W., and Lipman, D. J. (1990) *J. Mol. Biol.* **215,** 403–410
33. Hardin, C. C., Corregan, M., Brown, B. A., and Frederick, L. N. (1993) *Biochemistry* **32,** 5870–5880
34. Meyer-Siegler, K., Mauro, D. J., Seal, G., Wurzer, J., DeRiel, J. K., and Sirover, M. A. (1991) *Proc. Natl. Acad. Sci. U. S. A.* **88,** 8460–8464
35. Singh, R., and Green, M. R. (1993) *Science* **259,** 365–368
36. Nagy, E., and Rigby, W. F. C. (1995) *J. Biol. Chem.* **270,** 2755–2763
37. Shaffer, D. R., Brown, E. A., and Lemon, S. M. (1994) *J. Virol.* **68,** 5568–5578
38. Patton, J. G., Mayer, S. A., Tempst, P., and Nadal-Ginard, B. (1993) *Genes & Dev.* **5,** 1237–1251
39. Karpel, R. L., and Burchard, A. C. (1981) *Biochim. Biophys. Acta* **654,** 256–267
40. Jensen, D. E., Kelly, R. C., and von Hippel, P. H. (1976) *J. Biol. Chem.* **251,** 7215–7228
41. Hoagland, V. D., and Teller, D. C. (1969) *Biochemistry* **8,** 594–602
42. Constantinides, S. M., and Deal, W. C. (1969) *J. Biol. Chem.* **244,** 5695–5702
43. Minton, A. P., and Wilf, J. (1981) *Biochemistry* **20,** 4821–4826
44. Kawamoto, R. M., and Caswell, A. H. (1986) *Biochemistry* **25,** 656–661
45. Perucho, M., Salas, J., and Salas, M. (1980) *Biochim. Biophys. Acta* **606,** 181–195
46. Huitorel, P., and Pantaloni, D. (1985) *Eur. J. Biochem.* **150,** 265–269
47. Lin, T., and Allen, R. W. (1986) *J. Biol. Chem.* **261,** 4594–4599
48. Tsukiyama-Kohara, K., IIzuka, N., Kohara, M., and Nomoto, A. (1992) *J. Virol.* **66,** 1476–1483
49. Chang, K. H., Brown, E. A., and Lemon, S. M. (1994) in *Viral Hepatitis and Liver Disease* (Nishioka, K., Suzuki, H., Mishiro, S., and Oda, T., eds) pp. 132–135, Springer-Verlag, Tokyo
50. Andino, R., Rieckhof, G. E., Achacoso, P. L., and Baltimore, D. (1993) *EMBO J.* **12,** 3587–3598
51. Jackson, R. J., Hunt, S. L., Gibbs, C. L., and Kaminski, A. (1994) *Mol. Biol. Rep.* **19,** 147–159